

CHANGES IN CHEMICAL AND OPTICAL PROPERTIES OF THIN FILM METAL MIRRORS ON LDEF

Palmer N. Peters and James M. Zwiener
NASA/George C. Marshall Space Flight Center
Huntsville, AL 35812
Phone: 205/544-7728; FAX: 205/544-7754

511-27

John C. Gregory, Ganesh N. Raikar and Ligia C. Christl
University of Alabama in Huntsville
Huntsville, AL 35899
Phone: 205/895-6076, FAX: 205/895-6349

231

Donald R. Wilkes
AZ Technology, Huntsville, AL
Phone: 205/880-7481, FAX: 205/880-7483

SUMMARY

Thin films of the metals Cu, Ni, Pt, Au, Sn, Mo and W deposited on fused silica flats were exposed at ambient temperature on the leading and trailing faces of the LDEF. Reflectances of these films were measured from 250 to 2500 nm and compared with controls. The exposed films were subjected to the LDEF external environment including atomic oxygen, molecular contamination and solar ultraviolet. Major changes in optical and infrared reflectance were seen for Cu, Mo, Ni and W films on the leading face of LDEF and are attributed to partial conversion of metal to metal oxide. Smaller changes in optical properties are seen on all films and are probably caused by thin contaminant films deposited on top of the metal.

The optical measurements are correlated with film thickness measurements, x-ray photoelectron spectroscopy, optical calculations and in the case of Cu, with x-ray diffraction measurements. In a few cases, comparisons with results from a similar UAH experiment on STS-8 have been drawn.

INTRODUCTION

Earlier Results

The LDEF Experiment A0114¹ was designed to investigate the effects of atomic oxygen on orbiting spacecraft. Subsequently, degradation of surfaces was noted on early space shuttle missions and a dedicated part of mission STS-8 was carried out at a low altitude to further the investigations. Effects on optics were reported as part of the STS-8 results². The UAH portion of the EOIM-2 experiment flown on STS-8 was essentially a subset of the LDEF A0114 experiment in which approximately half of each sample surface was exposed with the other half covered by aluminum of the mounting plate, but unlike the free-flying LDEF, STS-8 had to be controlled to maintain the space shuttle's cargo bay in the orbital direction. To compare the effects resulting from the two missions properly, it is necessary to examine similarities and differences in parameters influencing both the experiments.

Mission and Sample Specific Effects

Due to a much longer exposure time, the total exposure to oxygen atoms for the LDEF leading surfaces was about 25 times that for the STS-8 surfaces; however, the rate (flux) of oxygen atoms was much higher on the lower altitude STS-8 surfaces. The initial reaction rates on virgin surfaces should correlate with the oxygen atom flux, which depends upon the atom density. The atom density depends upon the phase of the cyclic solar activity and the altitude of the orbit. The long term effects can be highly specific to individual samples as well as the mission. Some materials form such protective oxides that the predominant effect, if any, is a slight increase in oxide thickness. Other materials that form volatile species (e.g. osmium) erode rapidly, destroying thin films and producing roughness on bulk surfaces, which greatly modifies or destroys their optical properties. Materials forming nonvolatile but nonprotective oxides, such as silver, exhibit strong destructive surface changes which are more difficult to characterize, but for most optical applications these materials can be discarded. Nonreactive surfaces, such as gold, or those with protective oxides are the best candidates for optical applications. Contamination of these surfaces is a predominant cause of optical degradation, and the space environment can produce both desired and undesired effects on the optics. The vacuum induces outgassing of contaminants from spacecraft materials, but since the optical surfaces are initially well cleaned, transport to, and contamination of, the optics from other sources is more likely. The effect of atomic oxygen on deposited combustible contaminants such as hydrocarbons is to oxidize them into volatile species. However, many contaminants are from silicone-based materials, chosen for space applications due to their high mechanical stability and adhesive properties. These contaminants appear to be modified to form stable coatings after reaching the optical surfaces and being exposed to the space environment. Since silicone-based contaminants can greatly reduce atomic oxygen effects by providing a protective coating, it might be expected that the ratio of silicone contaminant deposition rate to atomic oxygen flux would be a factor in the overall effects. Sources of contamination and contamination transport to sensitive surfaces are complex issues⁵, and it is difficult to accurately predict rates of deposition. However, if contaminant depositions are similar at all altitudes and levels of solar activity, then missions initially carried out at high altitude during solar minimum (as with the LDEF) might experience greater subsequent protection from atomic oxygen due to contaminants than a mission carried out at low altitudes during solar maximum throughout the mission. Although later exposure of the LDEF at lower altitudes and higher solar activity provided most of the total fluence, earlier produced protective coatings could have had a strong influence on the later outcome of surface degradation, especially if surface renewal by heavy erosion or flaking did not occur. Such comparisons between STS-8, the LDEF, and other missions are needed and their results better understood to improve predictions of future effects.

Other Parameters

There are other factors that influence the comparison of the LDEF and STS-8 missions. The LDEF samples were prepared first, but were flown later, and exposed to ground-based environments longer than the STS-8 samples (the covered half of each sample acted as a control but it is difficult to isolate any ground-based effects). In both the experiments, thin films were deposited on optical flats to enable precise measurements of changes in film thickness using a stylus profilometer and to enhance optical measurements. However, while available $\sim \lambda/2$, flats of variable quality were used on the LDEF, uniformly superior optical flats were purchased later for STS-8. As a result better characterization of changes in film thickness was possible with the STS-8 samples. Contamination levels were generally more widespread on the LDEF samples than the STS-8 samples. Silicone-based contamination of <6 nm was observed from an isolated, nearly point source on only one STS-8 sample, while ~ 2 -5 nm contamination appears typical on our non-etched LDEF samples. Limited stability has been observed for a few of the effects of atomic oxygen; thus, measurements on some surfaces would be different in situ (in orbit) than after recovery and perhaps as a function of time after recovery. Also, some measurements, such as

observation with a scanning electron microscope, or other processes which deposit appreciable energy to the surface, can modify areas scanned on some sensitive atomic oxygen exposed samples. The importance of chronological order of measurements from least likely to more severely degrading has been better recognized after the STS-8 studies. These studies produced a few such modified effects and greater precautions have been taken to avoid such effects on the LDEF samples by dividing or shielding parts of the samples, if modification is anticipated.

SAMPLE PREPARATION

The deposited films were optically thin in many cases, with the thickness in the range of 20 to 100nm. An important effect of such thin films is that a very small change in film thickness represents a large percentage property change. As described below, much greater measurement precisions were obtained for stylus profilometry and optical transmission measurements by using films on the order of a few tens of nanometers thick. Ideally, both opaque, as well as such thin films should be used to separate out effects of the substrate in the optical properties and the possibility that thinner films might absorb more solar radiation and reach a higher equilibrium temperature while in orbit. Another advantage of opaque films, is that interface layers, such as chrome, can be put down to improve film adhesion to the fused silica substrates since the optical reflectance of an opaque film would not involve this interface; because of the increased difficulty of interpreting very small changes when additional layers are present, interface or buffer layers were not used with these transparent films. Although paints and smooth bulk samples were also flown, their properties are reported separately, only the effects on metal films deposited on optical flat are reported here.

A typical sample was prepared by cleaning a fused silica flat after verifying that it was flat to $\sim \lambda/2$ or better. Planar diode sputtering and e-beam evaporation were predominately used for in-house film depositions. Some of the coatings were obtained from external sources.

EXPOSURE

The samples were mounted in a 9 mm thick aluminum plate⁴. Flat bottom holes the diameter of the optical flats plus clearance were machined two-thirds of the way through from the back, and the front 3 mm thickness was machined so a "half-moon opening" exposed approximately one-half of the front surface of each sample, while elastomer disks or O-rings were compressed behind the 3 mm thick samples to hold the samples in place. Attempts to produce hot and cold plates dependent upon thermal control coatings and isolation of the hotter plate appear to have created such modest temperature differences that little evidence of any temperature effect was observed. Similar samples were positioned on the LDEF's C9 (leading) and C3 (trailing) surfaces. During free flight, only portions of the LDEF trunnions and scuff plates had any line of sight to the A0114 surfaces and their solid angles from the samples were small. Deployment and recovery effects were relatively small on C3 surfaces, but not negligible. Present estimates⁵ of the total fluence are 8.72×10^{21} for the C9 surfaces and 1.32×10^{17} for the C3 surfaces, with most of this total occurring in the last year, since the LDEF started much higher during a period of solar minimum and ended much lower during a period of solar maximum. Non-orbiting environmental exposure effects, if any, are much harder to quantify.

MEASUREMENT TECHNIQUES

Characteristics

As previously observed, exposure to atomic oxygen in orbit can effectively "thin" some metallic films while changing their optical properties. A material whose oxide evaporates (e.g., osmium) exhibits a huge loss in film thickness and has limited usefulness if exposed to atomic oxygen. Other films of interest for optical applications often exhibit very small changes in optical properties (a small increase in light transmission and a small decrease in reflectance for instance). Several factors could be responsible for the observed effect: extremely low loss of metal atoms due to very low probability formation of a volatile oxide or a very low sputtering yield, both of which would result in a small decrease in overall film thickness. Formation of a very thin, stable, transparent oxide can also similarly change the optical properties. However any metal oxide formed tends to increase the overall film thickness slightly, although the pure metal is effectively "thinned". An additional cause for the changes observed could be an overlying contaminant layer which would increase the overall film thickness without loss of "metal thickness". A combination of these factors may be present, and difficulties can be experienced in separating the causes of the effects. A variety of measurements have been performed, in addition to the optical measurements, to identify the causes where possible.

Stylus Profilometry

One measurement of choice for determining film thicknesses is stylus profilometry, which is independent of the sample's optical properties. Stylus profilometry measurements are complimentary to optical measurements, which may pose difficulty in determining film thicknesses accurately if the indices of refraction are inhomogeneous, have anisotropies or numerous unknown layers. We have experienced problems in many cases with single frequency ellipsometry measurements; more complex techniques will have to be used to satisfactorily measure these film thicknesses optically. Stylus profilometry has difficulties if the surface is not smoother than the precision desired, and longer range waviness can create problems if sharp steps in the thickness being measured are not present. Shadowing effects at mask edges generally produce too broad a step to measure very small changes in film thickness. We developed a technique for stylus measurements of film thicknesses that overcomes this problem if the film can be removed in fine scratches without damaging the substrate. Films relatively softer than fused silica can be removed over small regions by using a fine wire to scrape lines through the metal, leaving a bare substrate; uniform, flat bottoms are indicative of successful scratches. Each scratch produces a square well pattern in the stylus trace and multiple, parallel scratches in the film produce a "square-wave-type" pattern which can be modulated by waviness in the surface of the flat, but still provide precise thickness measurements, since the top to bottom of each scratch indicates uniformity in the film thickness. Softer intermediate hardness films in layers have even produced multiple step heights, with ledges at film interfaces and a flat bottom at the substrate. The precision is limited somewhat by surface smoothness, with average changes of less than 1 nm in thickness being detectable with high quality flats and very smooth films. It should be noted that the scratches are actually produced perpendicular to the mask edge of sufficient length that stylus traces perpendicular to the scratches and parallel to the mask edge can provide several measurements of thickness in both the exposed and covered areas to verify that the change is not due to a taper in the film thickness as deposited. Consistent differences in thickness measured between exposed and nearby unexposed areas can be attributed to exposure. Much poorer precisions result if poorly defined steps or chance pinholes in the films must be used to estimate the exposed and unexposed thicknesses, since surface waviness obscures the poorly defined steps and widely spaced pinholes may measure a small variation in original film thickness unrelated to exposure as well as exhibit poor steps. Some films were too hard to scratch without damaging the substrate; using patterned films may solve such problems in future experiments. The results of previously measured film thicknesses

are reported here to help interpret the optical changes. One artifact, recently determined, from these types of measurements will be described, however. To avoid spoiling the central region of the films, where optical measurements are performed, the scratches were made at the boundary between exposed and unexposed areas as far removed from the sample center as possible; one of the chosen locations was near the corners of the "half-moon shaped" exposed area on the straight section of the boundary. The straight boundary has the advantage of producing the sharpest step with least shadowing because this straight edge on the aluminum mask had a knife edge nearly in contact with the sample surface. To accurately define the mask boundaries before the samples were removed, two small very fine, V-shaped notches were produced with a diamond microscribe traced around each corner. When stylus measurements were made too close to these scribed markings, fine debris from the silica substrates appears to have produced a higher density of spikes in the stylus measurement than would otherwise occur. This can be incorrectly attributed to other sources of particles or changes in surface roughness that result in increased scattering of the optical surfaces. While some local debonding of an iridium film was observed and reported previously (no interface layer was used), the density of spikes observed in the stylus measurements was greater than the density of debonded points and may have been related to debris near the boundary marks where the stylus measurements were made. Why the iridium predominantly debonded in the exposed area in a fairly uniform pattern of microscopic crazed peaks is speculative; possibly this was due to greater stresses on the exposed film and would presumably be less likely if a chrome, or other, interface layer was first deposited on the substrate to produce better adhesion. It should be noted that adhesion, except at these spikes was good, however, since the remainder of the film was not easily removed by scratching or other techniques. The softer gold and also platinum films did not exhibit similar local debonding; although bonding of gold to the fused silica was undoubtedly poor, stresses in the gold film were most likely much lower.

X-Ray Photoelectron Spectroscopy

X-ray photoelectron spectroscopy⁶ was used to investigate the surface contamination and oxide species present on the exposed and unexposed surfaces of a number of samples. The unexposed region of each sample was used as control. The samples were mounted on the sample stub with double-sided tape. Mg ka or Al ka source was chosen for x-ray radiation. System pressure during analysis was $\sim 2\text{-}5 \times 10^{-9}$ Torr. A pass energy of 89.5 eV was used to acquire the survey scans from 0 to 1100 eV binding energy to identify various elements present on the surface. A pass energy of 17.9 eV was used for high resolution elemental scans for surface composition in terms of atomic percentage. The XPS core levels were measured with a pass energy of 8.95 eV to obtain chemical state information from the details of binding energy and peak shape. Sample charging was measured by the displacement of the adventitious surface C 1s peak at 284.8 (± 0.2) eV. Carbon 1s due to hydrocarbon contamination and oxygen 1s peaks due to oxide species plus other carboxyl and moisture contaminants can be easily differentiated. Enhanced levels of oxygen and other impurities and a decrease in the substrate peaks on the exposed areas compared to covered areas was one indication of exposure effects. Details of the spectra, such as extra peaks (including satellite peaks), peak broadening, energy shifts, and peak ratios can be interpreted in terms of oxides formed, their oxidation states and relative amounts of contamination, especially when different measurement angles are compared.

Optical Measurements

Four types of optical measurements have been performed on the samples reported: optical density measurements using a small area white light source with a scanning microdensitometer, diffuse optical density measurements over a 1 mm aperture using four broad band color filters, diffuse reflectance (from a 12.5 mm diameter area) versus wavelength from 250 nm to 2500 nm, and infrared emissivity measurements. Only the reflectances versus wavelength are reported in detail here. Ellipsometry measurements have been attempted on a number of samples, but so far

the results have been generally disappointing. Only the scanning microdensitometer provided good evidence of the relative uniformity of the films in the covered and exposed areas; however, its measurement did not resolve variations smaller than its spot size nor gradients along the optical path. The disappointing ellipsometry measurements suggest that such depth variations or perhaps inhomogeneities within the film plane smaller than the microdensitometer spot, exist and create some measurement problems.

Other Measurements

On some metals where appreciable, but incomplete, reaction occurred on leading exposed surfaces, it was practical to analyze the structure of the modified surface, using x-ray diffraction, but only when a thin film attachment was used. The results of this type of XRD measurement were most useful for copper, which showed intermediate reactivity.

RESULTS

Sample C3-04, tin, Trailing Edge

Stylus profilometry measurements, of the trailing edge (wake side) tin sample exhibited considerably less precision in the measured film thicknesses than for the leading edge (ram side) tin surface (see Table I). This result usually indicates a greater roughness in the measured surface. Although the film appears to be possibly thicker in the exposed area, the measurement precision is poorer than any suggested difference. XPS showed a higher concentration of Na in both exposed and covered areas, presumably due to NaCl contamination, sources of which are unknown. Si concentration was higher in the exposed area than in the covered area. Both C and O concentration was similar in both the areas.

The reflectance, Fig. 1, exhibits considerable improvement at shorter wavelengths (tin was the only film showing significant improvement) after exposure. Interestingly, improvement in reflectance is observed to be higher for the trailing tin sample than the leading tin sample. Although it is possible for some overcoats to enhance reflectance and hydrocarbon contaminant removal could accomplish the same result, no completely satisfactory explanation for these results is offered from the existing data.

Sample C9-04, tin, Leading Edge

Table I indicates that the exposed area of the leading tin sample had an apparent thinning. Table II shows that there were increases in oxygen and silicon, and a decrease in carbon in the exposed area. Carbon, from hydrocarbons (hydrogen is not observed), is a common atmospheric contaminant. Its decrease in the exposed area is consistent with removal by atomic oxygen; the remaining carbon in the exposed area could have come from post flight exposure. Traces of Na, Cl, and F may indicate minute amounts of salt contamination. The significantly higher levels of silicon and oxygen and much smaller level of tin in the exposed area indicates appreciable overlying contamination consistent with models assuming silicone contamination from the LDEF followed by modification of the surface, perhaps to silica, by the atomic oxygen. Again, a slight increase in reflectance in the exposed area is observed in Fig. 1; removal of hydrocarbon contamination could be a contributor to better reflectance, while the SiO₂-type contamination would presumably decrease the reflectance; however, appreciably greater hydrocarbon removal would seem necessary to explain the larger change in sample C3-04, which received the least oxygen; therefore other mechanisms are apparently involved.

Sample C3-09, tungsten, Trailing Edge

The tungsten film was too hard to be scratched effectively without damaging the silica substrates; therefore, only a thickness in the covered area is listed in Table I; such thicknesses are usually estimates based on deposition parameters and the best measurements permitted by stylus measurements of any pinholes in the film where dust particles resided during deposition.

In such cases where the scratching techniques were not applicable for determining changes in thickness of the exposed area, attempts were made to use stylus tracing from unexposed to exposed areas to look for a step at the mask boundary. The precision of such step measurements was strongly dependent upon finding a region with well-defined, reasonably sharp steps at the former location of a mask knife edge. Such satisfactory steps are found sometimes; this tungsten sample showed a step up of 18.6 (± 3.1) nm in going from the covered area to the exposed area of the sample. This might be interpreted as an increase in film thickness due to exposure, but substrate surface changes cannot be ruled out. Table II indicates a considerably lower percentage atomic concentration of tungsten for the exposed than the covered area, and considerably more Si, consistent with a silicone-based overcoat. The level of W measured would not be observed through 18.6 nm of overlying contamination. A "swelling" of the film by oxidation also seems unlikely, since this trailing film received minimal oxygen exposure and little difference in oxygen concentration is observed between exposed and covered areas by XPS. It would be easier to assume the 18.6 nm step was unrelated to exposure, if it were not for similar steps being observed on other samples independent of whether they were on leading or trailing surfaces. It should be noted that where actual film thicknesses were measured (by the scratch technique) that thickness changes were much smaller than these large steps. If the similar steps are indeed related to exposure, further studies are needed to determine whether the films, the fused silica substrate, or both are involved; the change is a much smaller percentage of the substrate thickness than the film thickness, and may be within the stability limits of fused silica under appreciable stresses for a long length of time (about 6 ppm change). The substrates were compressed on the holder for ~ 6 years. Regardless, it is premature to associate the larger measured steps with surface preparation, contamination, film swelling or any specific mechanism at this time. Calculated values for the reflectance of tungsten using literature optical constants gave results both higher and lower than we measured for covered tungsten, and the calculated values were more irregular than for other films.

Sample C9-09, tungsten, Leading Edge

The leading tungsten sample did not permit accurate stylus determination of its film thickness since there were no good pinholes nor other film thickness steps to measure. The thickness has been estimated to be between 60 and 70 nm. Again, a measurable, somewhat more precise, step of 19.4 (± 0.7) nm was observed in stylus traces from covered to exposed areas, which, within the precision of the measurements was the same as that observed on the trailing sample. It is assumed that this step also does not represent a contaminant thickness, since Table I shows the tungsten atomic concentration to be only slightly less in the exposed than the covered area. The reduction in carbon and increase in oxygen in the exposed area agrees with high fluences of atomic oxygen to the leading surfaces. The relatively large amount of Si concentration on the covered area as seen in Table II was not expected, nor understood, and is atypical. However, grains of silica debris or pinholes to the silica substrate in the analyzed area could account for higher Si. The fairly uniform reduction in reflectance at long wavelengths in Fig. 4 for the exposed area is not consistent with calculated effects of a thin overlying contaminant (see gold as such an example), but this and the high tungsten concentration are more consistent with appreciable tungsten oxide; this oxidation occurred to a lesser extent than for some of the other films, such as copper.

Sample C3-10, platinum, Trailing Edge

As would be expected, this trailing platinum film exhibited nothing attributable to oxidation. The precision of the stylus measurements of film thickness was relatively good in both covered and exposed areas; values of 38.4 (± 1.3) nm thickness in the covered and 43.6 (± 2.3) nm thickness in the exposed areas were obtained, as shown in Table I. The difference of ~ 5 nm is similar to changes on other films believed to be contaminated by films of silicone-based origin. However, the measured reflectance versus wavelength, as shown in Figure 5, shows no difference between covered and exposed areas, which is puzzling, since calculated reflectance changes for gold films with < 5 nm contaminant thickness are noticeable (as discussed later). Repeated measurements confirmed the same reflectances, and the stylus measurements were on the correct samples (note thickest Pt has highest reflectance). XPS showed a higher concentration of Si and O in the exposed area than in the unexposed area and vice versa is true for C (see Table II). This indicates formation of a thin layer of silica based on XPS chemical shifts. Other contaminants were found in very minute quantities.

Sample C9-10, platinum, Leading Edge

This leading platinum sample shows precise thickness measurements, with both covered and exposed areas indicating ~ 59 nm film thicknesses, as shown in Table I. This indicates no apparent contamination on the exposed area using stylus measurements, however, there is significantly more Si indicated on the exposed area from XPS measurements and the Pt is greatly reduced, as if overcoated, as shown in Table II. The same XPS measurements also show more carbon on the covered area, and presumably hydrocarbon contaminants were oxidized and removed from the exposed area. One seemingly unlikely explanation for no thickness change would be that the increase in SiO_2 was balanced by an equivalent removal of hydrocarbon.

The measured reflectances were consistently higher than those calculated using literature optical constants and the measured film thickness as shown in Fig. 6 ; a platinum film from another source measured in the middle of these sets of data. The XPS measurements on the C9-10 film definitely indicate contamination, similar to that observed later on gold, and the reflectance loss on the exposed area is similar to that for gold, but no completely satisfactory answer is offered for not having measured the contaminant by stylus, nor explaining a stylus measured increase for the trailing exposed surface with no reflectance change.

The platinum does differ from gold in that oxide layers may be contributing to the observed changes, but more details are needed to fit the platinum with a satisfactory model.

Sample C3-16, copper, Trailing Edge

Good to fair precisions were obtained for the film thicknesses on this trailing copper sample. Although ~ 0.8 nm increase in thickness of the exposed area film is suggested in Table I, this value is less than the precision of the stylus measurements for this sample. Table II shows slightly higher copper in the exposed area, little difference in oxygen, slightly less carbon, and a small increase in Si. Measured reflectances in both covered and exposed areas in Fig. 7 differ only at shorter wavelengths from calculated values, using literature optical constants and our stylus measured film thickness. Reflectance measurements on 1 year old copper films in our laboratory showed fairly good agreement with the literature. Some environmental degradation is suspected, even in the covered areas, after a decade, but we cannot verify this, since as-coated reflectances were not measured. The very small difference between covered and exposed area reflectances may be contaminant or oxide related, but all effects are too small for our measurements to be definitive.

Sample C9-16, copper, Leading Edge

The effects on the leading copper film were gross, as evident visually, since the exposed area no longer had a metallic appearance. Table I shows that this sample grew in thickness over 30 nm in the exposed area. X-ray diffraction using a thin film attachment, showed that copper oxide was formed and identified it, mostly as Cu_2O .⁷ However, pure copper and a trace of CuO were also present. Our best estimate was that the film consisted of the equivalent of ~ 92 nm of oxide and ~ 13 nm of copper; however, ellipsometry and other measurements so far have not provided any evidence of layers. The reflectance was greatly reduced, as shown in Fig. 8, and the transmission of light was much greater in the exposed area, as previously reported. Attempts to calculate reflectances using literature values of optical constants for copper and its oxides on fused silica gave no agreement; no combination of copper on silica covered by copper oxide gave the amount of reflectance loss observed. It appears that the converted film has its own optical constants and we believe that these are not uniform, perhaps having a gradient from the surface to the substrate, or at least having some distribution of copper within the oxide film. Any contamination effect seems negligible compared to the chemical changes on this sample; however, carbon is less and Si and oxygen greater in the exposed area. The higher Cu peak in the exposed area is associated with the Cu_2O .

Sample C3-24, molybdenum, Trailing Edge

Molybdenum was another film which did not scratch satisfactorily for thickness measurements. This trailing film was estimated to be 35.1 (± 4.3) nm thick in Table I, and only stylus traces from unexposed to exposed areas were available to estimate any changes in the surface. Again, a large 18.6 (± 3.1) nm, step was observed, which is still not considered contamination, and is not satisfactorily explained. This film is estimated to be nearly the same thickness as for C9-24, but it shows considerably less reflectance, Fig. 9, than the covered area of C9-24, Fig. 10. XPS measurements showed considerable Si contamination in the exposed area which has converted into silica. There was hardly any Si in the covered area. However there was a large increase in N concentration in the covered area which is difficult to explain. It is hypothesized that the molybdenum films may have been deposited with oxide incorporated; this could explain the reduction in reflectance of covered films compared to calculated values.

Sample C9-24, molybdenum, Leading Edge

The leading molybdenum sample also could not be scratched, but its thickness was estimated to be 35.4 (± 1.9) nm, in Table I. Stylus traces from the covered to exposed areas did not give detectable steps, but a yellow-green color on the exposed area suggests an oxide interference. The absence of detectable steps indicates that they were not very sharply defined at the mask boundary compared to the substrate surface variations. Table II, shows appreciable oxygen and carbon in the covered area, suggesting appreciable oxidation of the original film plus hydrocarbon contamination. Appreciable carbon was removed by the ram oxygen in the exposed area; since residual carbon is seen on the numerous other samples exposed to ram oxygen, it may result from postflight exposure as opposed to carbides, etc. Considerably more Si and additional oxygen are present, consistent with contamination on the LDEF, but the effects of oxidation are considered to be the dominating factor. As discussed later, it is believed that initial oxide incorporation could have occurred in some of the films during deposition, lowering their reflectances compared to values calculated from literature constants, and the ram exposure further reduced the reflectance, as in Fig. 10.

Sample C3-45, nickel, Trailing Edge

The thicknesses of the nickel films were poorly known, since no suitable steps were obtained for film thickness measurements. The best estimate for the thickness, which was poor, was ~ 40 nm. Based on this thickness and literature values for the optical constants, calculated reflectances were found to be considerably higher than the measured reflectances, as shown in Fig. 11. Better agreement is obtained for considerably thinner films, but we believe that the nickel is thicker than necessary to obtain reasonably good agreement, suggesting that even the covered areas of the film contain more oxide than the nickel of the literature. Table II shows a smaller concentration of Ni in the exposed area of C3-45, indicating some contaminant overcoat, Si-based film being likely, with some reduction in the total carbon. The slightly higher oxygen could be associated with partially converted Si, but the uniformly small decrease in reflectance of the exposed area is more typical of slight oxidation of the nickel film.

Sample C9-45, nickel, Leading Edge

Table II shows that the ram side nickel film has a higher Ni concentration in the exposed than in the covered area; this appears to be characteristic of the heavier oxidized films where the metal concentration is associated with its oxide. The carbon is significantly reduced, as expected from the ram atomic oxygen removing hydrocarbons. The Si and oxygen are both also increased in the exposed area consistent with Si-based contamination and perhaps oxygen modification. The major decrease in reflectance of the exposed, ram nickel film in Fig. 12, however, is believed to be a result of increased oxidation of the nickel film.

Sample C3-46, gold, Trailing Edge

The modeling for the trailing gold sample is similar to that for the leading gold, which is discussed next in greater detail, because more results have been measured for it. The stylus profilometry results in Table I indicate that the film thickness for the covered area was 33.3 (± 0.5) nm and for the exposed area it was 35.3 (± 1.3); from the following discussion for C9-46, this thickness difference suggests that ~ 2 nm of contamination was acquired on C3-46 and XPS measurements seem to support this assumption (see Table II). The same model as for C9-46 can be used. It appears that roughly one-half as much contamination was acquired on C3-46 as on C9-46. From Fig. 13 it is seen that the reflectance loss is correspondingly less for the exposed C3-46 than the exposed C9-46 area in Fig. 14.

Sample C9-46, gold, Leading Edge

Fortunately, there are fewer parameters influencing gold than most materials. Two primary modes of degradation are apparent for the gold: (1) thinning of the film by physical sputtering, and (2) effects of contamination. Although gold has a high sputtering yield compared to most materials, the ~ 5 eV impact energies of oxygen atoms and higher energies for N₂ and heavier molecules, due to the orbital velocity, do not provide enough momentum exchange to produce significant sputtering. On STS-8 the fluence levels were below those needed to detect any effect of sputtering. McKeown⁸ reported sputtering of gold at levels less than 5×10^{-6} atom/molecule of the upper atmosphere striking the gold; the measurements were performed with quartz oscillators on Discoverer satellites with a perigee of ~ 200 km and ~ 10 eV particle-surface interaction energies (more typical of N₂). With atomic oxygen dominating the fluence at higher orbits the gas-surface interactions should produce even less sputtering yield. Using 5×10^{-6} atom of Au/atom of O multiplied by 8.72×10^{21} atoms of O/cm² for the total fluence produces 4.36×10^{16} atoms of Au/cm², as a conservative upper limit for the amount of gold that might be sputtered. Using the bulk density of gold, its atomic weight, and Avogadro's number, it can be shown that this amount

of sputtering would correspond to an upper limit of 7.4 nm thinning of the gold film. The slightly lower density associated with most films compared to bulk could increase the thickness sputtered slightly. Table I shows, from stylus measurements, that C9-46 had a film thickness of 31.7 (± 0.6) nm in the covered area and 35.4 (± 0.4) nm in the exposed area. This increase in thickness is assumed to be from contamination, and the XPS measurements in Table II support this conclusion, since the gold peak is greatly reduced, as if overcoated, and the Si and O peaks are much higher in the exposed than the covered area. The reflectance of C9-46, in Fig. 14, shows a decrease at short wavelengths. If we assume, for lack of better optical constants, that 3.7 nm of SiO₂ represents the contaminant on 31.7 nm of gold on a fused silica substrate, then the reflectances calculated using literature optical constants⁹ for pure gold and gold plus the SiO₂ are shown in Fig. 15. The loss in reflectance thus calculated represents a large fraction of the loss measured. If we assume that a loss in hydrocarbon contamination (C was much less in Table II) was made up by additional SiO₂, then it appears feasible to explain most of the total loss, if not all, as being due to contamination; the assumption of optical constants of SiO₂ might be slighting the calculated reflectance for the given contaminant thickness also. Although an increase in thickness of the exposed film was measured, rather than a thinning, it is still desirable to estimate the effect of sputtering, since any thinning could be overcompensated for by contamination thickening. Figure 16 shows the measured reflectances of C9-46 for the covered and exposed areas and calculated reflectances for two gold thicknesses: a 31.7 nm film thickness (covered area) and an assumed gold film thickness of 24.2 nm, which would result if 7.5 nm of gold had been sputtered from this film as an upper limit. Note that the measured reflectance of the covered area agrees with the literature, but the assumption of 7.5 nm thinning of the gold totally disagrees with the measured reflectance of the exposed area; not only is the reflectance at 250 and 300 nm wavelength not reduced by thinning, while the measured change is greatest there, but the thinning reduces the reflectance at longer wavelengths, where no change is measured. Lack of apparent sputtering may be explained in two ways: (1) the sputter yields are, as expected, even lower than the already very low upper limit on the yield, and (2) contaminants prevented, or greatly reduced, any sputtering that might have ordinarily taken place. Thus, the effects on the gold are rather well-modeled by assumptions of no sputtering and the presence of several nanometers of contamination.

CONCLUSIONS

A wide range of effects from atomic oxygen interaction with low Earth orbiting satellites occurs on metal films. Such films have numerous applications to electrical circuits, to thermal control coatings and to various optical systems; degradation of the physical, electrical, or optical properties of the films can be disastrous to mission objectives under some circumstances.

For very sensitive materials such as osmium, and silver, which have been previously reported^{10,11}, the effects of oxygen atom ram exposure are so severe that the use of these materials should be questioned unless great care is taken to protect the materials. The effects on films reported here, while less severe, still vary from possibly insignificant to unacceptable in terms of application and optical degradation. The films appear to be separable into those which are relatively insensitive to atomic oxygen, such that contamination probably dominates any effects, and those which are oxidized appreciably, causing their optical constants to be changed enough to challenge their use if exposure to ram oxygen is permitted.

In the insensitive materials category gold represents the best modeled material reported here. Measured optical properties of gold agreed well with accepted literature values; its reflectances, film thicknesses, and other measurements supported a model which discarded physical sputtering effects, at least for this LDEF mission, and attributed the smaller changes in the optical properties to a few nanometers of contamination. This contamination was apparently silicone-based and perhaps specific to this mission, but with the potential of being generated on

many missions because of the wide spread use of silicone compounds for space applications. Evidence of slightly higher Si contamination and degradation of the leading surfaces compared to the trailing was observed, but otherwise these samples were relatively insensitive to position on the satellite relative to the ram; if contamination had been limited to hydrocarbons, the ram facing surfaces would probably have been slightly improved in optical properties by removal of such contaminants, but the oxygen appears to have reacted with the silicone-based contaminants to form a more permanent film, perhaps similar to SiO₂. While a similar model was attempted with other films exhibiting small effects, probably because of thin protective oxides, not all of the measurements gave agreement. The results indicate that refinements are needed in measurements, interpretations, and modelling, especially as the number of parameters influencing the film properties increases over those for gold.

Those films more sensitive to oxidation appear to also acquire the same contamination, but the degradations are so dominated by the effects of metal oxidation that the sample's position relative to the ram direction becomes increasingly more important because of the sample's susceptibility to damage. The most extreme degradation reported here was also one of the best characterized sensitive materials, namely copper. The predominant features of the sensitive materials are small changes to the trailing films and large reflectance losses across a broad wavelength range for leading surfaces, associated with metal oxidation. The optical properties of these oxides, however, do not appear to be similar to those produced under equilibrium conditions for thermally grown oxide films. Problems with using ellipsometry and other optical methods of characterization to model these films suggest that perhaps variable concentrations of free metal may be distributed within the oxides, or at least the oxides do not provide uniform optical constants distributed in layers that are easily interpreted.

There is evidence that contamination by the modified silicone-based materials offers some protection from atomic oxygen degradation. The amount of protection of course would depend upon the contamination thickness and film integrity. Since rates of contamination and fluxes of atomic oxygen to the surfaces are strongly mission dependent, it is advisable to not only account for anticipated fluences of atomic oxygen, but also levels of contamination that might be expected for a given mission; the latter effects can utilize extensive studies of outgassing properties of materials that have been studied, but the transport mechanisms associated with depositing the contaminant on various surfaces and the fixation processes need to be studied in greater detail.

REFERENCES

1. Gregory, J.C.; and Peters, P.N. The Interaction of Atomic Oxygen with Surfaces at Orbital Altitudes, *The Long Duration Exposure Facility (LDEF)*, Clark, L.G, Kinard, W.H., Carter, D.J., and Jones, J. L., ed.: NASA SP-473, 1984.
2. Peters, P.N.; Gregory, J.C.; and Swann, J.T.; Effects on Optical Systems from Interactions with Atomic Oxygen in Low Earth Orbits, *Applied Optics*, **25**, 1290-1298 (1986).
3. Jemiola, J.M.; ed; *Proceedings of the USAF/NASA International Spacecraft Contamination Conference*, AFML-TR-78-190, NASA-CP-2039, March 1978.
4. Gregory, J.C.; and Peters, P.N.; Interaction of Atomic Oxygen with Solid Surfaces at Orbital Altitudes, *Proceedings of the First LDEF Mission Working Group Meeting*, NASA Langley Research Center, P.48, 1981.

5. Bourassa, R.; and Pippin, H.; Model of Spacecraft Atomic Oxygen and Solar Exposure Microenvironments, *Proceedings of LDEF Materials Results for Spacecraft Applications Conference, Oct 27-28, 1992*.
6. Chastin, Jill.; ed: *Handbook of X-ray photoelectron Spectroscopy*, 1992, Perkin-Elmer Corporation.
7. G.N. Raikar, J.C. Gregory, P.N. Peters, *Oxidation of Copper by Atomic Oxygen*, accepted for publication by **Oxidation Of Metals** 1994.
8. McKeown, D.; Surface Erosion in Space; *Rarefied Gas Dynamics*; ed: Laumann, J.A.; Academic Press, pp.315-326, 1963.
9. Palik, E.D.; ed: *Handbook of Optical Constants of Solids*, Academic Press, 1985.
10. Peters, P.N.; Linton, R.C.; and Miller, E.R; Results of Apparent Atomic Oxygen Reactions on Ag, C, and Os Exposed during the Shuttle STS-4 Orbits, *Geophysical Research Letters*, **10**, 569-571, 1983.
11. Gull, T.R.; Herzig, J.F.; Osantowski, F.F.; and Toft, A.R.; Low Earth Orbit Environmental Effects on Osmium and related Optical Thin-Film Coatings, *Applied Optics*, **24**, 2660-2665, 1985.

Table I. Measured film thicknesses and solar absorptances

A0114 SAMPLE*	MATERIAL	FILM THICKNESS		SOLAR ABSORPTANCE	
		COVERED, nm	EXPOSED, nm	α_s †	α_s †
				COVERED	EXPOSED
C3-04	TIN	131.3 ± 3.7	136.1 ± 6.3	0.311	0.295
C9-04	TIN	125.0	121.4 ± 0.6	0.313	0.295
C3-09	TUNGSTEN	52.2 ± 2.2	#	0.427	0.420
C9-09	TUNGSTEN	60.0 to 70.0	#	0.430	0.485
C3-10	PLATINUM	38.4 ± 1.3	43.6 ± 2.3	0.271	0.271
C9-10	PLATINUM	58.9 ± 0.9	60.7.0 ± 0.1	0.259	0.271
C3-16	COPPER	70.8 ± 1.0	71.6 ± 2.6	0.290	0.297
C9-16	COPPER	71.5 ± 7.2	105.8 ± 0.6	0.368	0.857
C3-24	MOLYBDENUM	35.1 ± 4.3	#	0.506	0.516
C9-24	MOLYBDENUM	35.4 ± 1.9	#	0.453	0.689
C3-45	NICKEL	#	#	0.571	0.583
C9-45	NICKEL	#	#	0.568	0.676
C3-46	GOLD	33.3 ± 0.5	35.3 ± 1.3	0.268	0.275
C9-46	GOLD	31.7 ± 0.6	35.4 ± 0.4	0.275	0.288

Notes:

* C3=Trailing edge (wake side), C9=Leading edge (ram side).

The C3-exposed surfaces received an estimated 1.32×10^{17} oxygen atoms/cm² total fluence.

The C9- exposed surfaces received an estimated 8.72×10^{21} oxygen atoms/cm² total fluence

See text for details

† The solar absorptance measured by the AZ Technology LPSR-200 spectro-reflectometer is actually (1-Reflectance) over the solar emission band. For thin films which are partially transmitting: (1-Reflectance) = Absorptance + Transmittance. Thus the values of α_s given here may not be the same as for solid metal (and should be quite different in the cases of C-9 exposed Cu, Mo, Ni and W.)

Table II: XPS Data for LDEF Thin Metal Films

Sample	Material	Side	Surface Atomic Concentration in %													
			Sn	W	Pt	Cu	Mo	Ni	Au	O	C	Si	Na	Cl	F	N
C3-09	Sn	Exposed	4.5							28.3	52.7	7.1	5.4	0.4	0.7	1.0
		Covered	13.1							24.6	53.7	2.7	4.0	0.5	0.4	0.9
C9-04	Sn	Exposed	2.7							54.3	15.3	25.2	1.3	0.3	0.4	0.6
		Covered	14.9							24.6	52.7	2.8	3.3	0.4	0.6	0.7
C3-09	W	Exposed		5.3						43.2	31.7	12.7	nd	nd	nd	7.0
		Covered		11.2						37.7	36.7	2.9	nd	nd	nd	11.5
C9-09	W	Exposed		9.5						48.8	16.2	16.7	0.3	0.4	0.6	7.3
		Covered		11.7						27.2	38.1	12.0	0.4	0.2	0.5	9.9
C3-10	Pt	Exposed			9.4					47.7	18.0	19.9	0.3	0.7	nd	3.9
		Covered			25.0					16.7	40.3	8.5	1.1	1.8	nd	6.6
C9-10	Pt	Exposed			4.9					51.0	18.2	21.0	0.7	0.7	nd	3.9
		Covered			14.3					23.6	46.4	6.5	0.5	0.7	0.3	8.1
C3-16	Cu	Exposed				8.7				23.9	62.9	5.4	nd	0.9	nd	nd
		Covered				5.5				23.3	66.8	3.6	nd	1.1	nd	nd
C9-16	Cu	Exposed				4.3				37.4	44.4	13.9	nd	nd	nd	nd
		Covered				2.7				21.6	65.8	9.3	nd	0.6	nd	nd
C3-24	Mo	Exposed					4.0			46.9	24.7	15.2	0.4	0.2	1.2	7.4
		Covered					12.2			36.3	32.2	0.9	1.0	0.3	0.6	16.3
C9-24	Mo	Exposed					7.9			48.7	25.6	17.8	nd	nd	nd	nd
		Covered					19.6			38.0	39.1	3.3	nd	nd	nd	nd
C3-45	Ni	Exposed						4.3		36.2	47.8	10.0	nd	0.5	1.6	nd
		Covered						10.5		27.8	58.9	2.0	nd	0.7	tr	nd
C9-45	Ni	Exposed						14.7		54.6	13.2	15.4	nd	nd	2.2	nd
		Covered						12.6		34.5	45.7	6.3	0.5	0.4	nd	nd
C3-46	Au	Exposed							16.5	41.0	19.7	16.5	0.4	0.5	nd	5.3
		Covered							42.2	12.7	34.4	6.3	0.2	0.4	nd	3.7
C9-46	Au	Exposed							4.5	56.4	15.6	22.0	tr	0.9	0.8	nd
		Covered							22.9	18.8	54.7	2.5	3.0	0.3	1.0	nd

Note: nd= not detected, tr=trace

C3-04, TIN

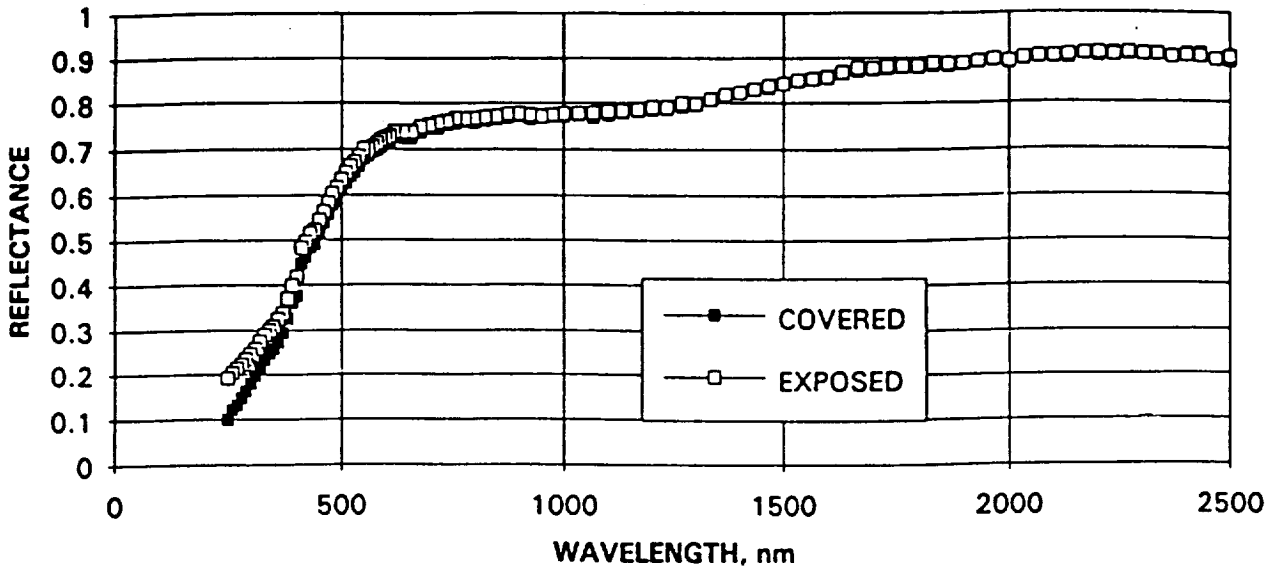


Fig. 1 Reflectances of covered and exposed areas on the trailing (wake side) tin film.

C9-04, TIN

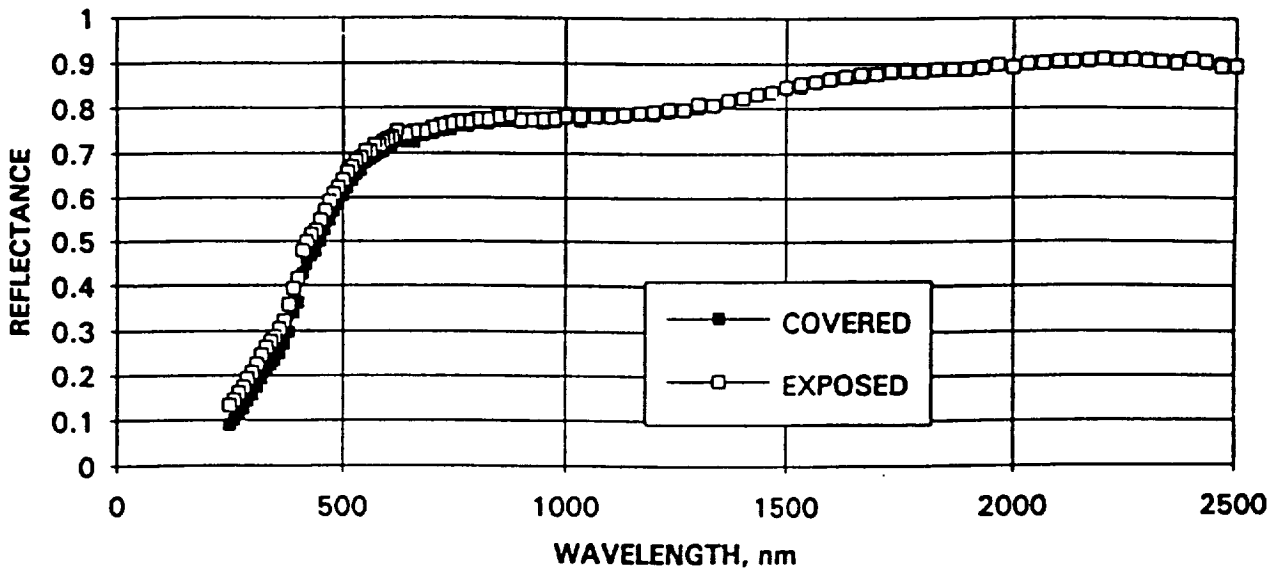


Fig. 2 Reflectances of covered and exposed areas of the leading (ram side) tin film.

C3-09, TUNGSTEN & CALCULATIONS

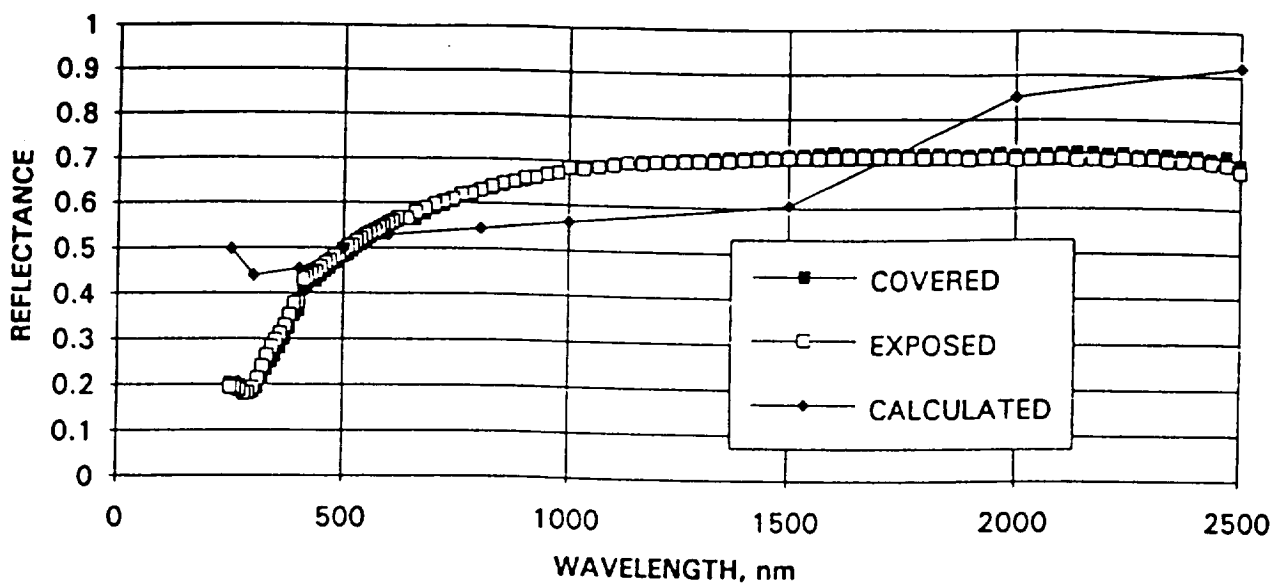


Fig. 3 Reflectances of covered and exposed areas of the trailing (wake side) tungsten film and calculated reflectances using the measured film thickness and optical constants from the literature.

C9-09, TUNGSTEN

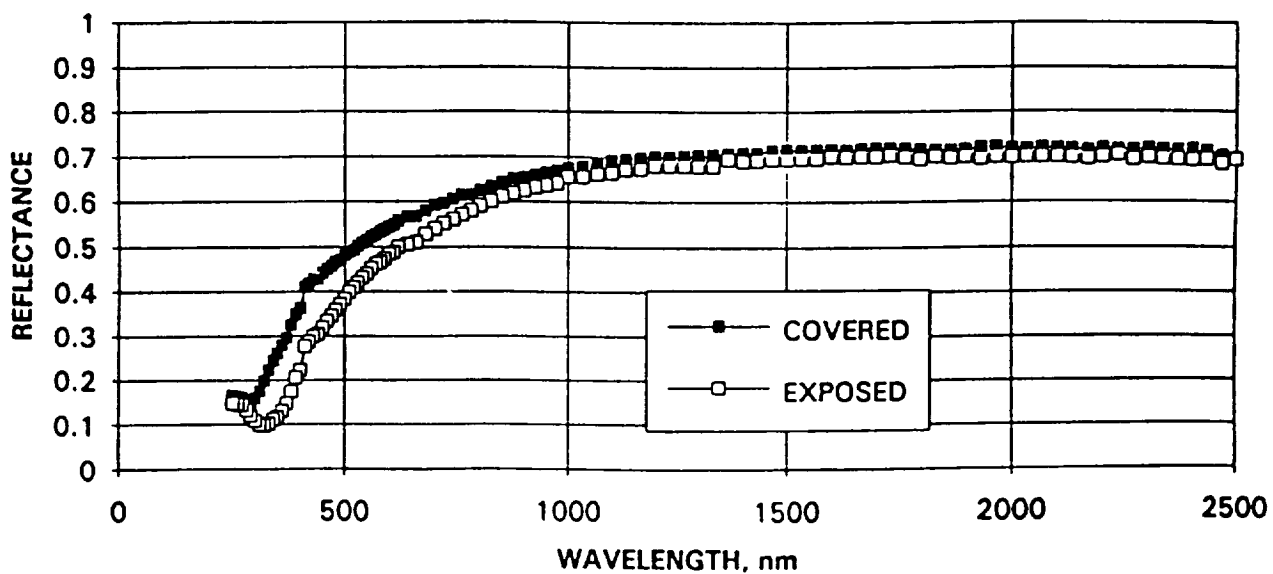


Fig. 4 Reflectances of covered and exposed areas of the leading (ram side) tungsten film.

C3-10, PLATINUM

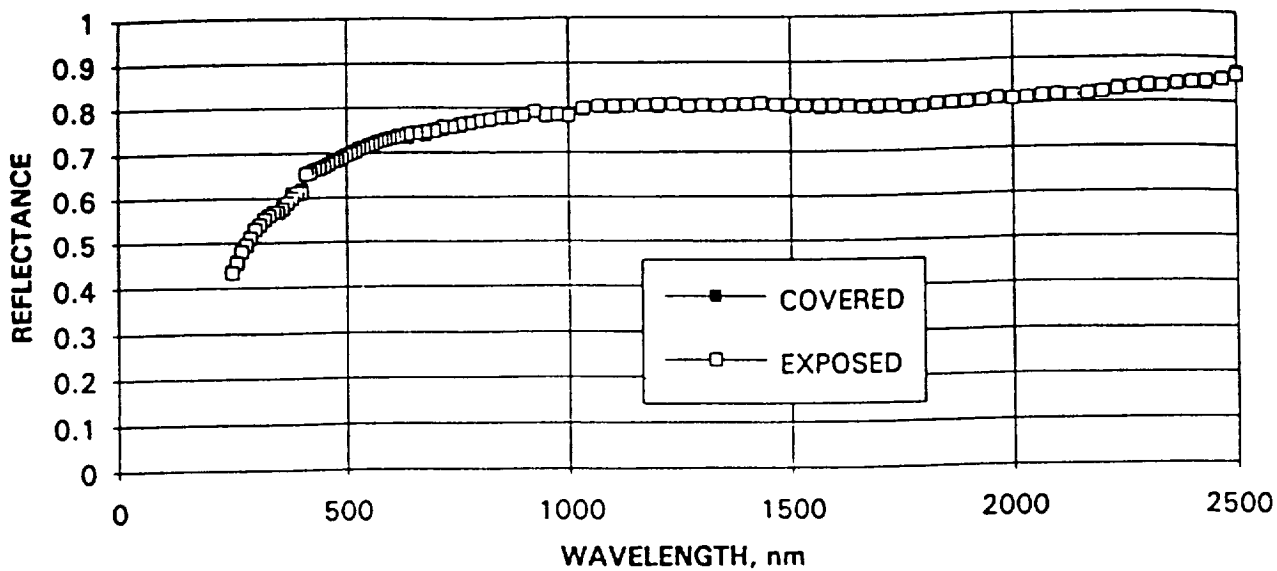


Fig. 5 Reflectances of covered and exposed areas of the trailing (wake side) platinum film.

C9-10, PLATINUM & CALCULATIONS

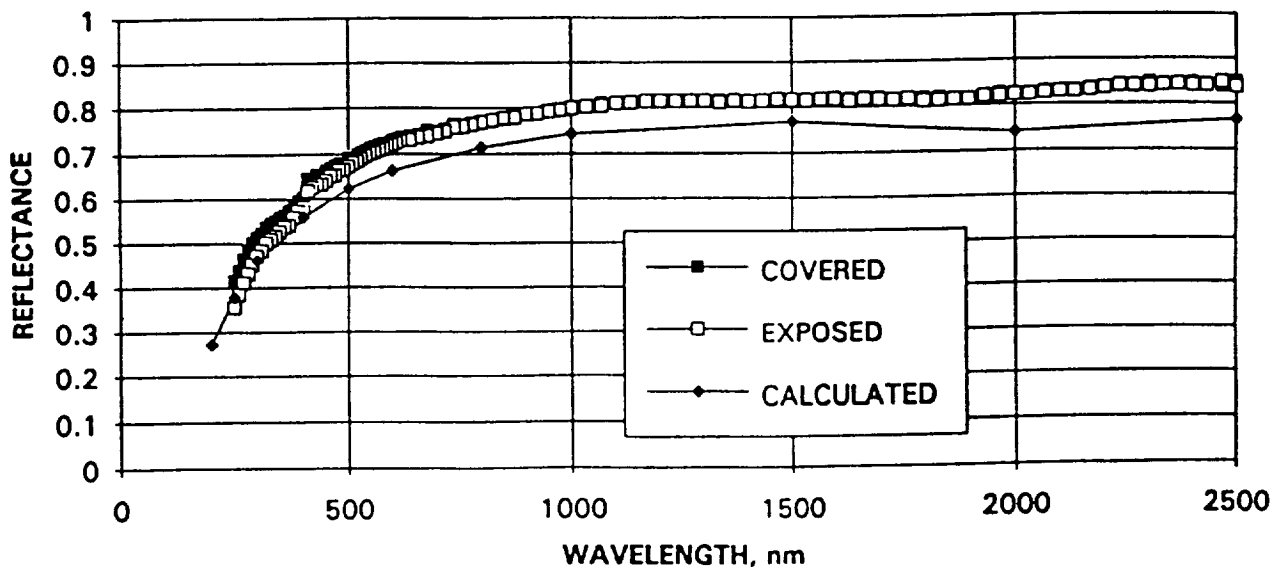


Fig. 6 Reflectances of covered and exposed areas of the leading (ram side) platinum film and calculated reflectances using the measured film thickness and optical constants from the literature.

C3-16, COPPER

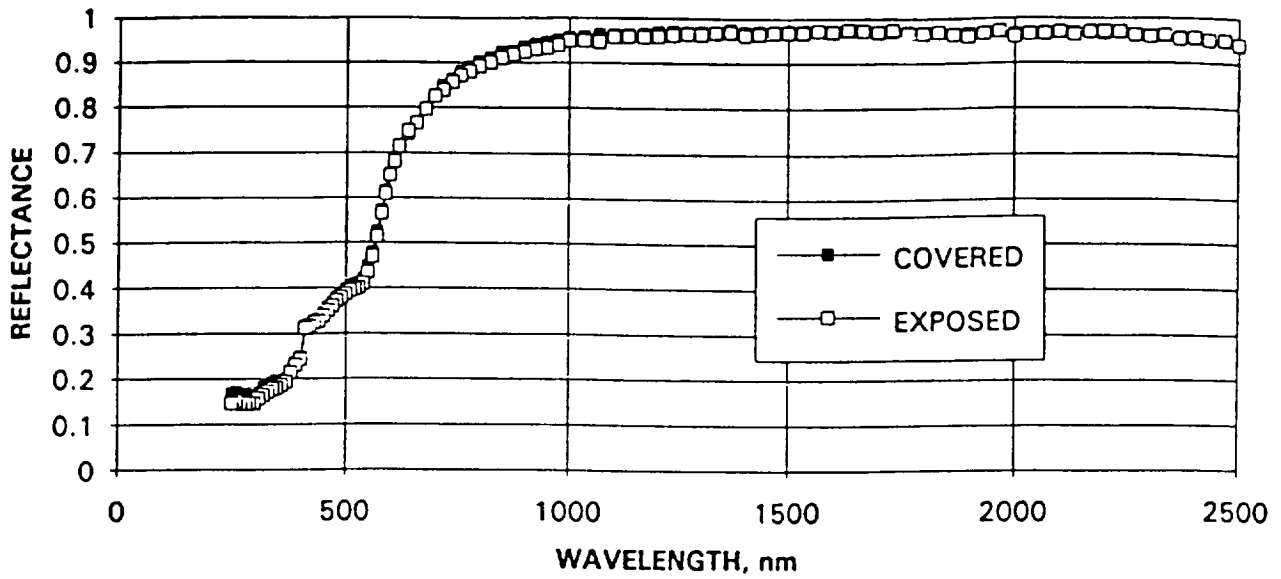


Fig. 7 Reflectances of covered and exposed areas of the trailing (wake side) copper film.

C9-16, COPPER

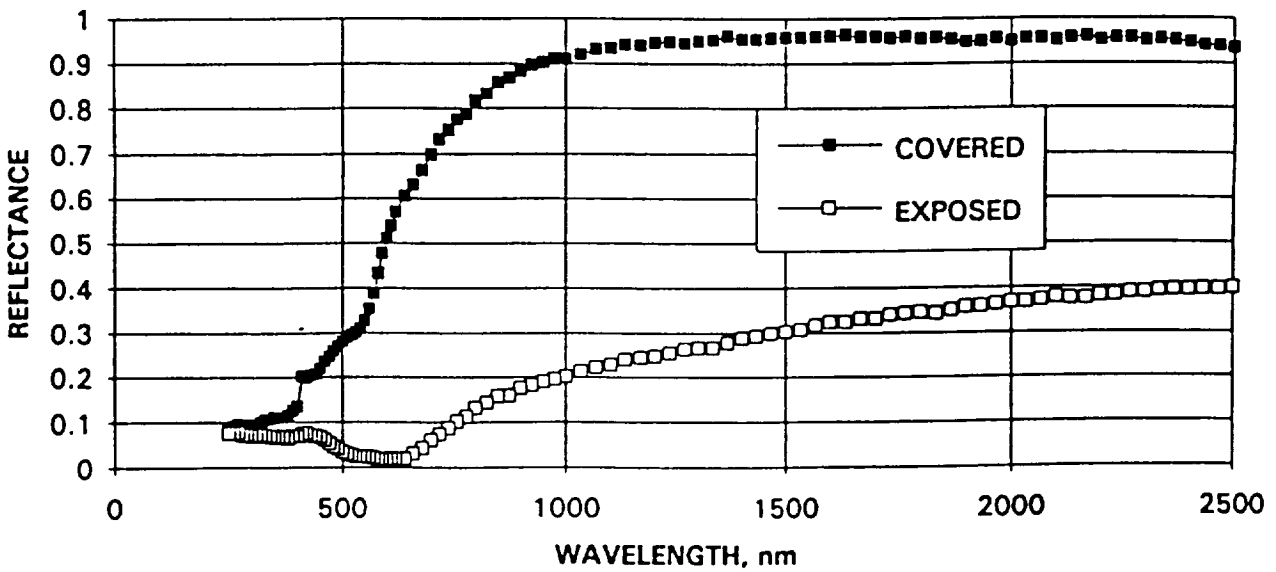


Fig. 8 Reflectances of covered and exposed areas of the leading (ram side) copper film.

C3-24, MOLYBDENUM

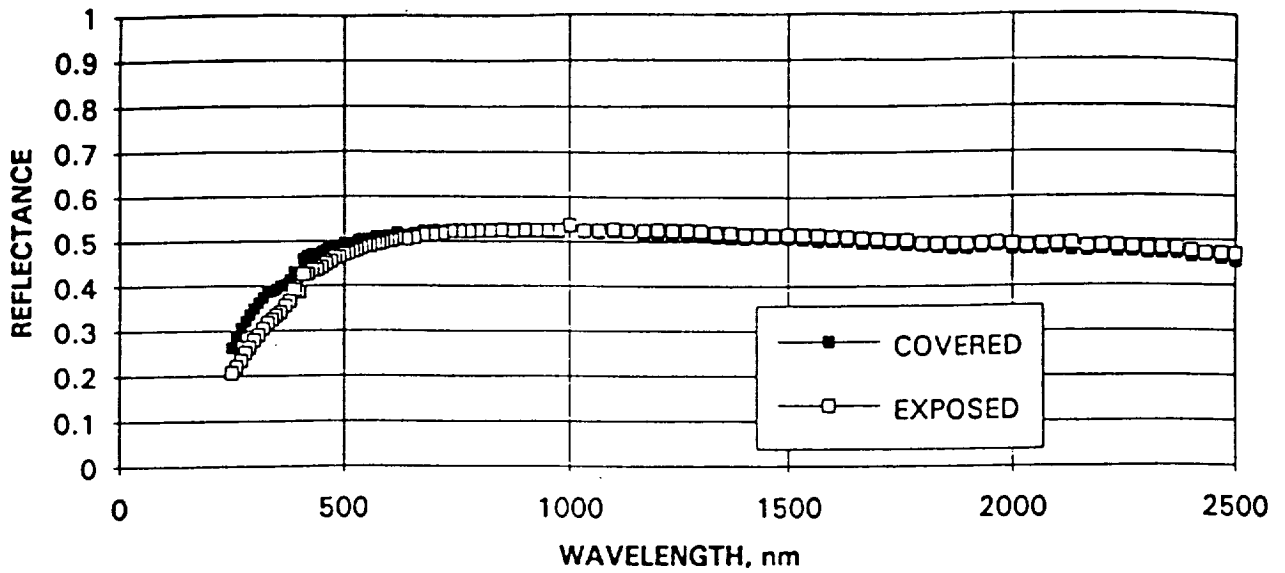


Fig. 9 Reflectances of the covered and exposed areas of the trailing (wake side) molybdenum film.

C9-24, MOLYBDENUM & CALCULATIONS

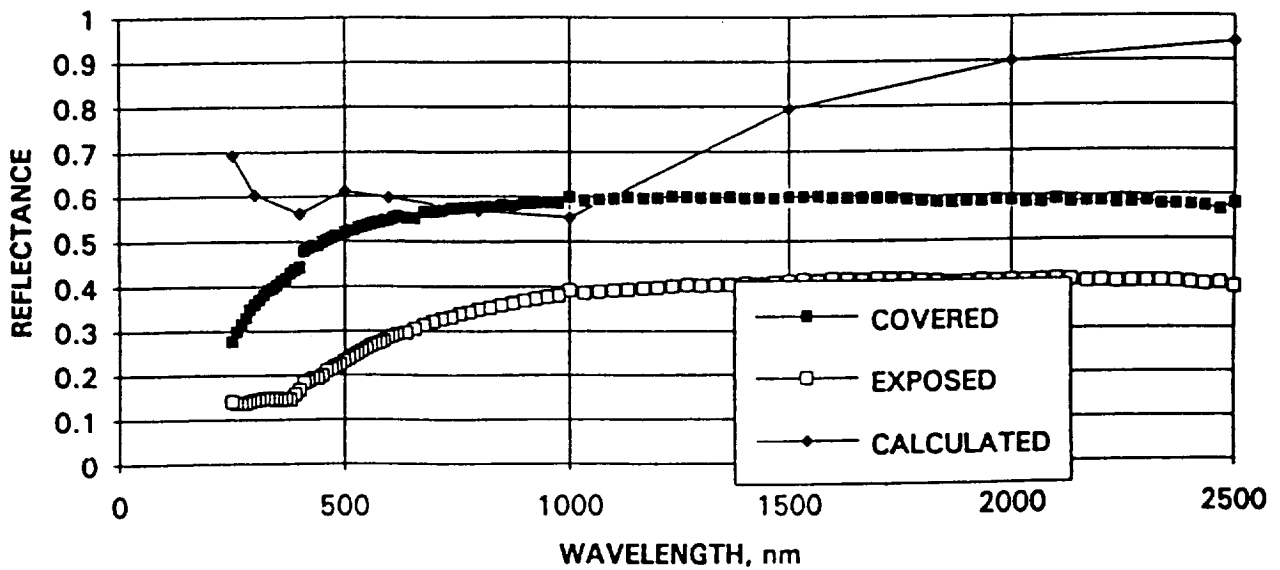


Fig. 10 Reflectances of the covered and exposed areas of the leading (ram side) molybdenum film and calculated reflectances using measured thickness of covered area and optical constants from the literature.

C3-45, NICKEL & CALCULATIONS

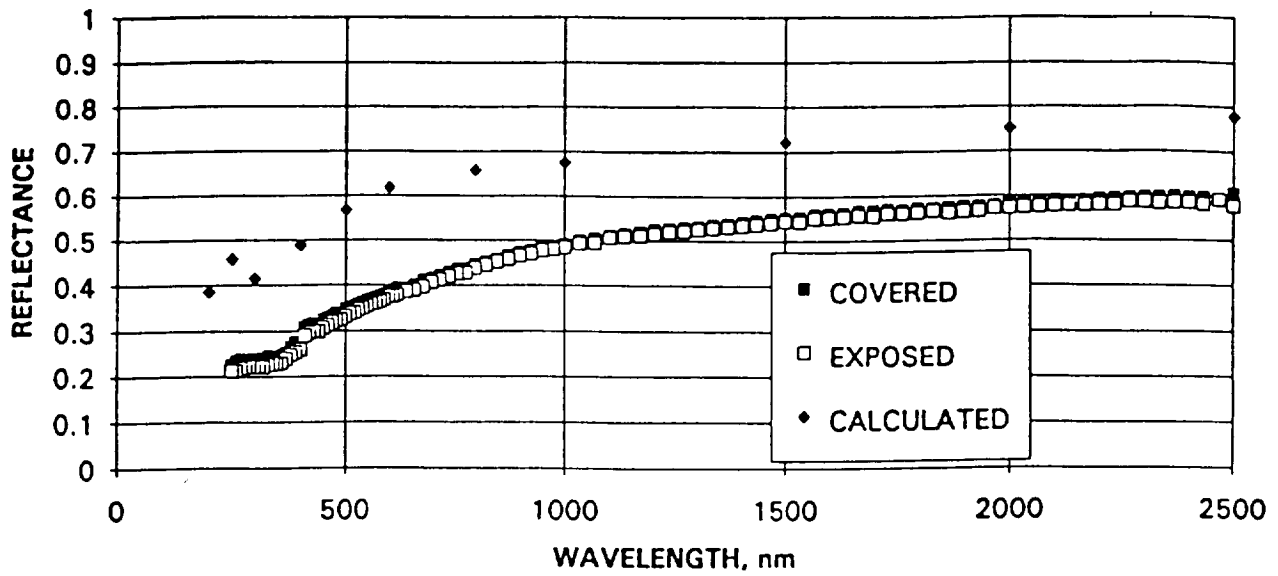


Fig. 11 Reflectances of covered and exposed areas of the trailing (wake side) nickel film and calculated reflectances using 40 nm film thickness (see text about uncertainty) and optical constants from the literature.

C9-45, NICKEL

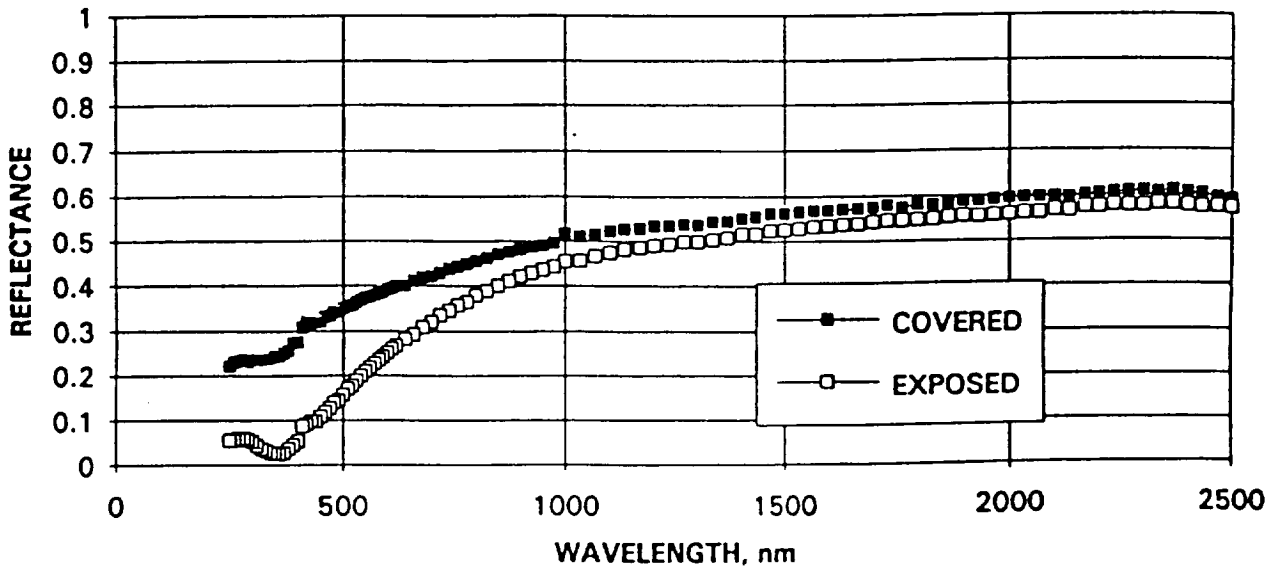


Fig. 12 Reflectances of covered and exposed areas of the leading (ram side) nickel film.

C3-46, GOLD

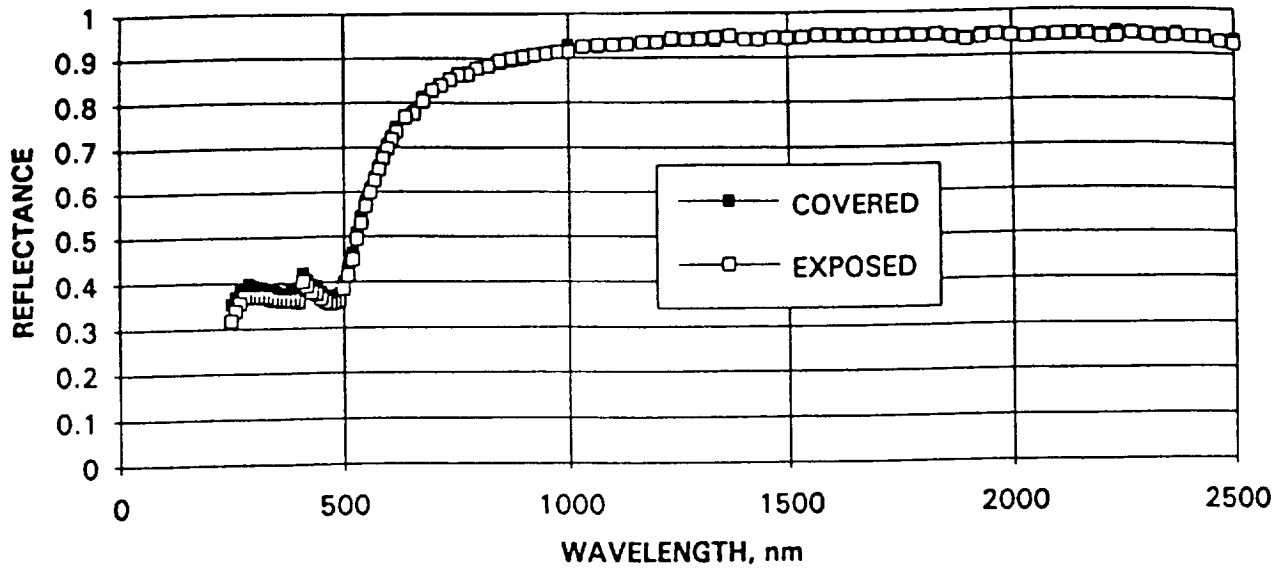


Fig. 13 Reflectances of the covered and exposed areas of the trailing (wakeside) gold film.

C9-46, GOLD

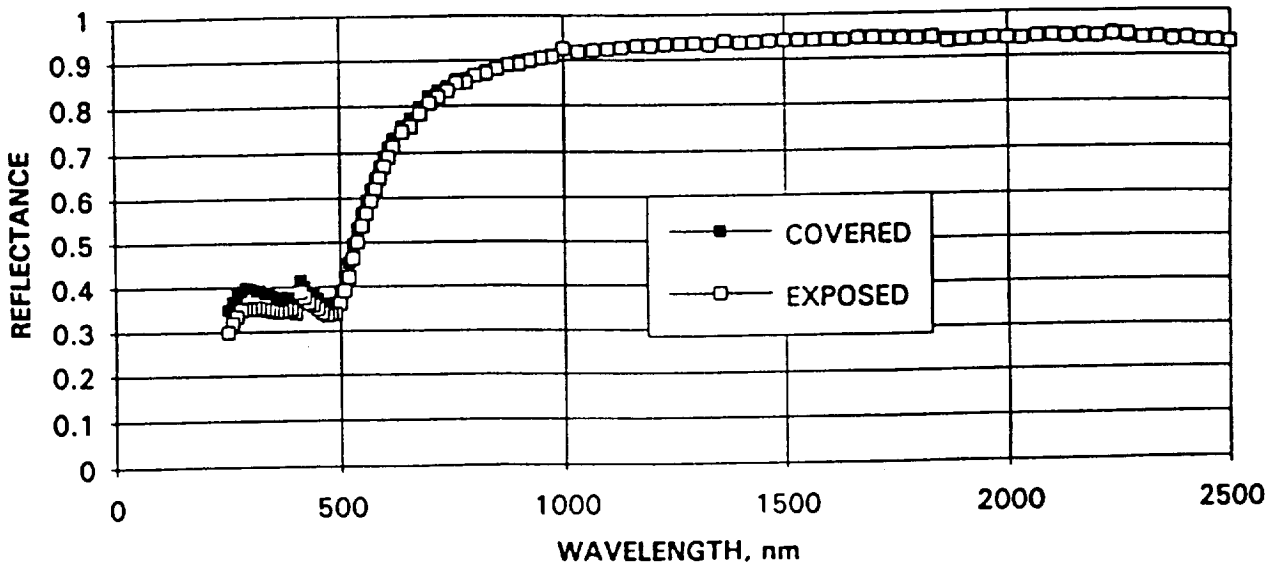


Fig. 14 Reflectances of the covered and exposed areas of the leading (ram side) gold film.

GOLD CALCULATIONS

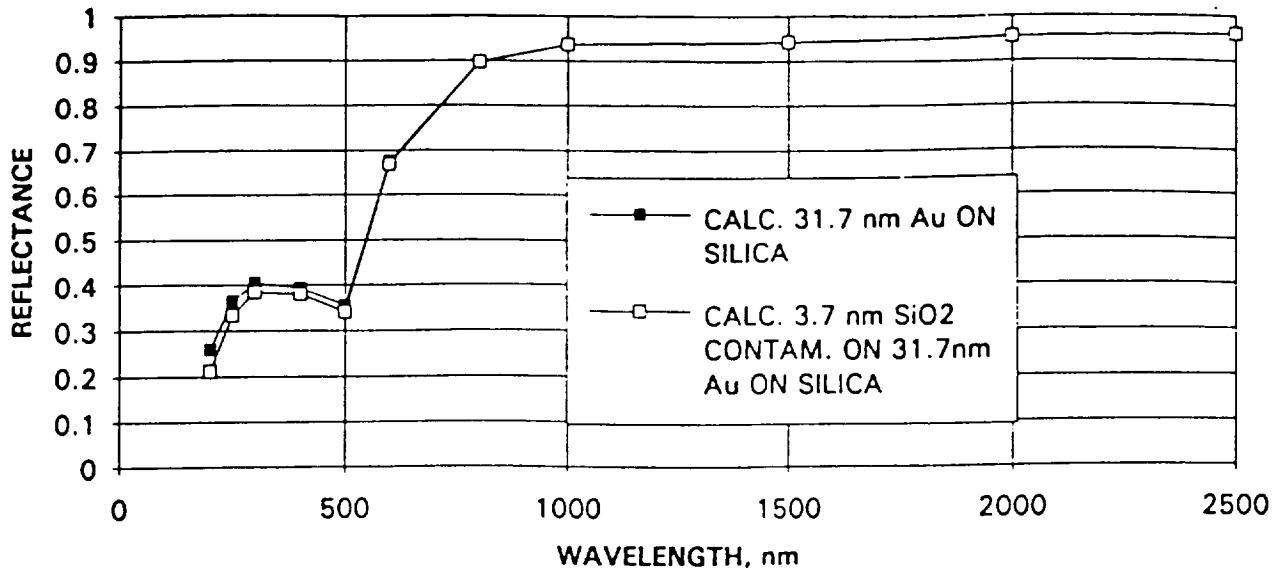


Fig. 15 Calculated reflectances of a gold film of 31.7 nm thickness and same film with 3.7 nm thickness of SiO₂ contamination on top; both on fused silica substrate.

C9-46, GOLD AND SPUTTER CHECK

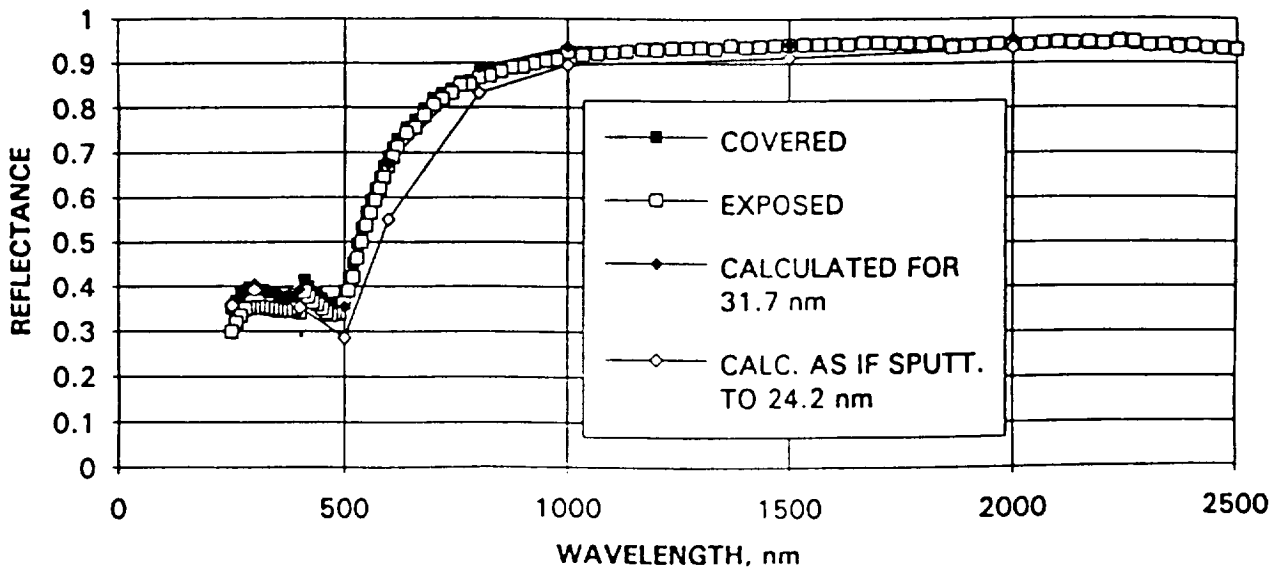


Fig. 16 Measured reflectances of covered and exposed areas of the ram side gold film compared to calculated reflectances of 31.7 nm and 24.2 nm gold film thicknesses; thinner gold would result if upper limit placed on sputtering occurred.

